OPTIMIZATION OF THE ENERGY PERFORMANCE OF MULTIPLE-SKIN FACADES

Dirk Saelens[1,*], Bert Blocken[1,2], Staf Roels[1], and Hugo Hens[1]
[1]Laboratory for Building Physics, Dept. of Civil of Civil Egineering,
K.U.Leuven, Kasteelpark Arenberg 40, 3001 Leuven, Belgium
[2]Building Envelope Performance Laboratory, Concordia University,
Dept. of Civil, Building and Environmental Engineering, Montreal, Canada
[*]Corresponding author: dirk.saelens@bwk.kuleuven.be

ABSTRACT

This paper describes how the energy performance of single storey multiple-skin facades can be optimized by changing the settings of the facades and HVAC-system. The energy performance is analyzed with a yearly whole building energy analysis under Belgian climatic conditions. Three multiple-skin facades are scrutinised: a mechanically ventilated airflow window, a naturally ventilated double-skin facade and a mechanically ventilated supply window. Their performance is compared against the performance of a traditional cladding with exterior and interior shading device. It is shown that both the heating and cooling demand may significantly be improved by implementing control strategies such as controlling the airflow rate and recovery of air returning from multiple-skin facades.

INTRODUCTION

The sensibility for environmental friendly and energy conscious building design urges the need to develop new facade technologies. In the search towards energy efficient and visually attractive facades, multiple-skin facades (MSFs) are regularly presented as being valuable solutions to follow the desires of modern architecture. MSFs (also known as active envelopes, second-skin facades, etc.) consist of two panes separated by a cavity through which air flows. The driving force for the airflow is natural or mechanical ventilation. In the cavity, usually a shading device is provided. Generally, distinction is made between naturally and mechanically ventilated MSFs. Extensive literature on MSF-typologies can be found in Compagno (1995), Oesterle et al (2001) and Poirazis (2004).

In literature, researchers provide advanced models to simulate specific MSFs. They, however, rarely couple the envelope level results to a building energy simulation program (Manz and Simmler, 2003, Safer et al, 2004). Only some combinations of MSF-modelling and building energy simulation are available. Most of these papers are restricted to only one MSF-typology. Müller and Balowski (1983) for instance analyze airflow windows, Oesterle et al (2001) give a comprehensive survey of double-skin facades and Haddad and Elmahdy (1998) discuss the behavior of supply air windows. Recent studies have recognized that an optimal control strategy combined with an overall building analysis is necessary to increase the overall energy efficiency (Saelens, 2002; Gratia and De Herde, 2004; Stec and van Paassen, 2005).

In this paper, the energy efficiency of an office equipped with three MSF-typologies is discussed and optimized. First, the building geometry and different models are presented. Then, different optimization strategies are derived and implemented. Finally, the results are compared against the energy performance of optimized traditional solutions.

CASE DESCRIPTION

Three MSFs and two traditional cladding systems are analyzed. The first MSF is a airflow window (AFW) (Fig. 1a). The outer glass is an argon filled low emission glass (U-value = 1.23 W/(m².K), g-value = 0.59). The shading device is a roller blind which is positioned in the cavity (α = 0.83, ρ = 0.09, τ = 0.08). The inner glass is a normal clear float glass (U-value = 5.67 W/(m².K), g-value = 0.85). The cavity is mechanically ventilated with interior air. The second MSF is a naturally ventilated double-skin facade (DSF) (Fig. 1b). The outer glass is a normal clear float glass. The same shading device is used and is also positioned in the cavity. The inner glass is a similar argon filled low emission glass. The cavity is ventilated with exterior air. The third MSF is a supply window (SUP) (Fig. 1c). The glass configuration is similar as for the DSF, but the cavity is now mechanically ventilated with exterior air. The traditional cladding systems have an argon filled low emission glass with the same properties as for the MSFs. The shading device is an exterior (IGUe) (Fig. 1d) or interior (IGUe) (Fig. 1e) similar roller blind.

These five facade systems are used in a narrow office building. The main facades have a north-east and south-west orientation. Figure 2 shows a section of a typical floor with an AFW. The facade consists of an opaque part that covers the false ceiling zone (h = 0.75 m) and a transparent part that runs from the floor to the false ceiling (h = 3.25 m). The false ceiling contains the HVAC supply and return ducts.

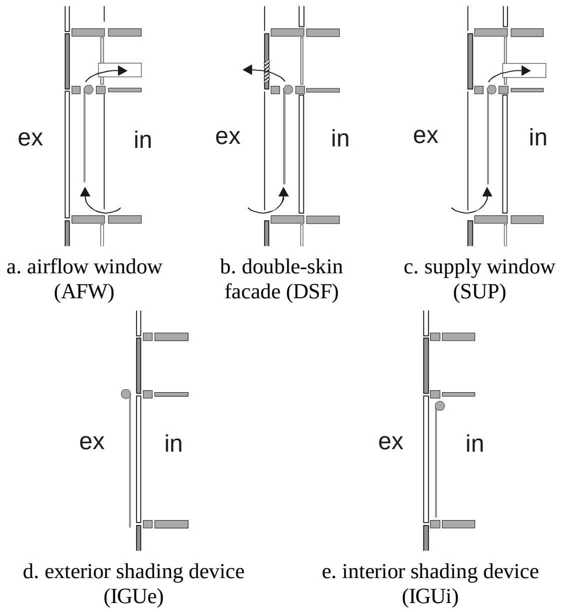

Figure 1 Schematic representation of the multiple-skin facades and the traditional solutions.

The floor is subdivided in three zones: a north-east external zone, an internal zone and a south-west external zone. Each zone has a depth of 4.50 m. In the analysis, the load or energy demand is presented as an average per unit of office floor. It is defined as the energy needed to keep the office temperature between the setpoints. The energy demand includes the ventilation energy, control inefficiencies and distribution losses or gains of the air ducts. It excludes the energy needed for fans nor does it take into account the efficiency of the HVAC-plant.

The setpoint temperature for heating is 21 °C with a night set-back to 16 °C. The setpoint temperature for cooling is 26 °C with a night set-back to 35 °C. The office hours run from 7 a.m. till 7 p.m.. The set-back is also enabled during the weekend. To maintain the temperatures between the setpoints a PID controller sensing the operative temperature of each zone is used. The operative temperature is defined as a weighted average of the air temperature and mean surface temperature. Weighting factors are 0.55 and 0.45 respectively. Internal gains due to occupancy, lighting and office appliances are split into a

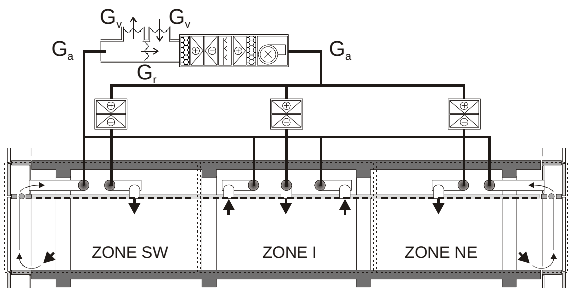

Figure 2 Schematic representation of the simulated office floor for a typical AFW configuration.

convective and radiative part according to the ASHRAE-guidelines (ASHRAE, 1997). The convective gains are added to the air temperature, the radiative gains are distributed over the internal surfaces proportional to the surface area. The air handling unit provides heating and cooling. Furthermore the offices are equipped with cooled ceilings, which is a common feature in offices with MSFs. All simulations use the climatic conditions of the Test Reference Year of Uccle, Belgium.

MODELING

To analyze the energy demand, a modelling environment combining a model of the facades, a model of the office zones, a model of the heating and cooling system and a model of the building energy management system has been developed.

All models are combined into a commercially available dynamic building energy simulation program (BESP) TRNSYS 15.3 (2000). The thermal behaviour of the MSFs and traditional facades is calculated with a cell centred finite volume method which is described in Saelens (2002).

Figure 3 shows the connection between the facade model and the office zone for the mechanically ventilated airflow window. The MSF-model passes the inner pane average surface temperature ($T_{s,MSF}$), the cavity exhaust air temperature ($T_{out,MSF}$) and the total transmitted solar energy (I_{MSF}) to the BESP. The latter is distributed over floor area (q_s in Fig. 3). The simulation program in turn provides the MSF-model with the incident direct ($I_{b,t}$) and diffuse ($I_{d,t}$) solar radiation, the angle of solar incidence (α), the zone air ($T_{a,3}$) and average surface temperature (part of $T_{star,3}$), the exterior air ($T_{a,e}$) and the sky temperature (T_{sky}). Saelens et al (2004) stress the importance of modelling the inlet temperature on the energy performance of MSFs. Similarly, a correct modelling of the outlet temperature is important in cases where the return air of the multiple-skin facade is to be reused. Therefore the inlet (zone 1 in Fig. 3) and outlet zone (zone 2 in Fig. 3) are modelled separately. Saelens et al (2004) also stress the importance of taking into account the gains and losses from the supply and return duct in the false ceiling. These losses and gains are accounted for in the false ceiling zone (zone 4 in Fig. 3) in which the HVAC return and supply ducts are placed.

In case of the traditional solutions, the inlet and outlet zone are not ventilated. The treatment of the surface temperature and the incoming solar radiation remains the same. When the shading is lowered, the interior or exterior temperature acts as inlet temperature for the naturally ventilated cavity. In case of the interior shading device, the extra heat source from the air flowing out of the cavity is added to the convective gain of the office zone ($q_{gain,3}$ in Fig. 3).

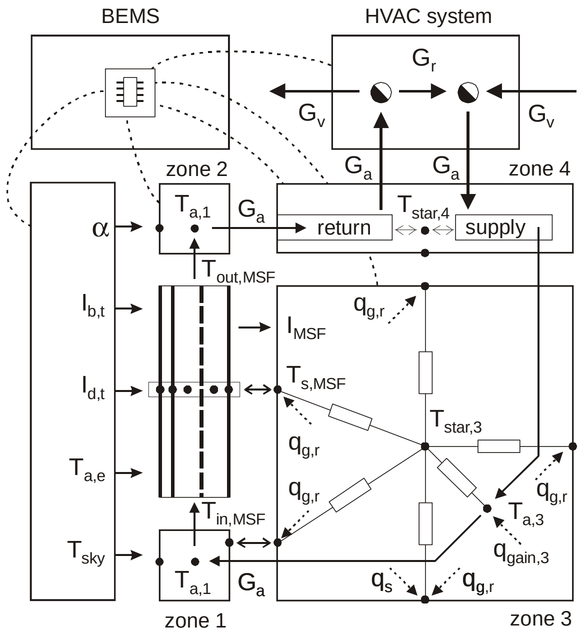

Figure 3 Implementation of the AFW-model into the Building Energy Simulation Program.

OPTIMIZATION STRATEGIES

Energy efficiency is an important argument to choose MSFs as facade concept. MSF-systems are presented as being superior to traditional facades both during the heating and the cooling season. The energy efficiency objectives obviously depend on the MSF-typology. Nevertheless, two main principles can be distinguished: (1) MSFs may reduce the transmission losses in winter and the gains in summer and (2) MSFs can either expel the return air to avoid overheating or reuse the return air in order to use the absorbed solar energy and recover some of the transmission losses.

In the non-optimized cases, the cavity ventilation of the mechanically ventilated MSFs (AFW and SUP) equals the hygienic ventilation rate (G_a = G_v = 20 m³/(h.m)). The airflow rate (G_a) through the naturally ventilated cavity (DSF) depends on the weather conditions and varies with time. As for the traditional cladding systems (IGUe and IGUi) the office zones are mechanically ventilated with the hygienic ventilation rate (G_v). During night-time and weekends the airflow rate is set back to a minimum airflow rate which equals half the required ventilation rate.

Analyzing the heating demand results (QH in Table 1), the IGUe shows to be the most energy consuming solution. Nevertheless the traditional solutions – which have the highest transmission losses – are not really outperformed by the AFW and DSF. Much can be attributed to the differences in solar gains. Compared to the IGUe, the IGUi has an 8 % lower heating demand due to the position of the roller blind at the inside. This produces higher indirect solar gains. The direct solar gains of the MSFs are considerably smaller than that of the IGUs because of the extra pane. For the DSF this compensates for the lower transmission losses. The inner pane of the AFW has a lower thermal resistance than that of the DSF and moreover the AFW is ventilated with interior air, which results in even lower transmission losses. As a consequence the heating demand is about 20 % lower compared to the IGUe. Because of the preheating of the ventilation air, the SUP outperforms all other variants and requires roughly half the heating energy needed by the other facade solutions.

The cooling demand (QC in Table 1) strongly depends on the indirect solar gains. Despite the higher direct solar gains, the IGU with exterior shading device (IGUe on Fig. 4b) has the lowest cooling demand. The best option to reduce to indirect gains is to prevent the solar radiation from entering the building. The IGU with interior shading device (IGUi) not only has a high direct solar gain but also suffers from high indirect solar gains. As a result it consumes 55 % more cooling energy than the IGUe. The AFW does not perform much better. It has lower direct solar gains compared to the IGUs and it also has lower indirect gains than the IGUi. However, the higher overall insulation level prevents the building to cool down during night-time. As a result, the AFW only performs somewhat better than the IGUi. The DSF is able to approach the performance of the IGUe as it has an inner pane with high thermal resistance. This prevents the absorbed solar radiation from entering the office. The SUP has the poorest cooling performance and requires 2.5 times more energy than the IGUe. The advantage of preheating the ventilation now becomes a major disadvantage.

Table 1
Energy demand of non-optimized facades.

ENERGY DEMAND (KWH/(M².A))					
case	**IGUe**	**IGUi**	**AFW**	**DSF**	**SUP**
QH	38.0	35.3	31.6	36.2	17.9
QC	-17.8	-39.2	-36.9	-19.8	-45.3

Unfortunately, most MSF-typologies are incapable of lowering the heating and cooling demand simultaneously. Only by combining typologies or by changing system settings according to the particular situation, a substantial overall improvement over the traditional solutions is possible. This implies that control mechanisms are inevitable to make MSFs work efficiently throughout the entire year. Two important optimization strategies for MSFs are identified and will be explored and implemented here. Where possible, both strategies will be combined to achieve an optimal solution.

(1) *Airflow rate control.* The airflow rate in the office zones as well as in the MSF-cavities may be changed to improve the energy efficiency. According to the facade typology these changes may not be

independent. For the AFW and the SUP there is a relation between the overall building airflow rate and the airflow rate through the MSF-cavity. For the DSF, the cavity airflow rate may be independent of the airflow rate through the office zones. Changing the airflow rate will also be used to allow free cooling of the building.

(2) *Recuperation of the return air*. The air passing through a MSF-cavity is heated by transmission losses through the inner pane and by impinging solar radiation. During heating conditions it may be interesting to use the return air as an energy source to heat the building. Some facade typologies use the MSF-cavity as a heat-exchanger to preheat the ventilation air. During cooling conditions there is no need to recover energy. Instead, the hot air returning from the MSF-cavities is preferentially expelled.

Airflow windows (AFW)

We discuss four strategies to improve the energy efficiency of AFWs: (1) a fixed change of the cavity airflow rate, (2) a controlled change of the cavity airflow rate, (3) recuperation of the return air and (4) a combination of airflow rate and recuperation control.

Let us first analyze the influence of the airflow rate assuming that the airflow rate is fixed throughout the entire simulation. In principle the three office zones are treated independently. As a consequence the zone airflow rate normally equals the cavity airflow rate. In this analysis we also consider what happens if the return air from the internal zone (Zone I on Fig. 2) is distributed towards the external zones. This distribution increases airflow rate in the external zones and the AFW-cavity by 50 %. There is no recuperation in the HVAC-system: the recuperation airflow rate (G_r in Fig. 2) equals zero.

An increase of the cavity airflow rate increases the cavity temperature and reduces the transmission losses. As long as the airflow rate does not exceed the total ventilation rate of the building, an increase of the cavity airflow rate is favourable to lower the heating demand. This is illustrated by the reduction of the heating demand for the cases with distribution compared to the cases without distribution (Table 2). If the total AFW airflow rate exceeds the total buildings ventilation rate (i.e. 20 $m^3/(h.m)$), extra exterior air has to be inserted into the building. The heating of this extra air has a higher energy cost than the reduction of the transmission losses. Therefore, an optimal situation is achieved when the airflow rate through the facades equals the total ventilation airflow of the building. In such a way, AFWs are used as a heat exchanger for the exhaust air.

In summer, an increase of the airflow rate helps to lower the cooling demand. Two effects are important: (1) the reduction of the indirect solar gains due to the increased airflow in the AFW and (2) the free cooling effect by increasing the exterior ventilation. Comparison of the results with and without distribution of the internal zone return air indicates that the latter is far more important.

The airflow rate based on the ventilation rate is the most favourable option to reduce the heating demand. In summer, it is favourable to increase the airflow rate to lower the cooling demand. As a consequence it is useful to implement a controller which chooses an optimal airflow rate according to the energy needs. By using a speed controllable fan or adjustable diaphragms in the air ducts, the controller is able to change the airflow rate of each zone separately. The decision of the airflow rate controller is based on the energy mode of a particular zone. If a zone is in heating mode, the ventilation airflow is set. If a zone is in cooling mode, the maximum airflow rate is set as long as the exterior temperature is lower than the setpoint for cooling. The definitions of heating and cooling mode should be carefully chosen. Monitoring of the energy demand in the terminal units of a particular zone for instance may result in an instable and non-optimal behavior. An example illustrates this. If the temperature of a particular zone surpasses the setpoint for cooling, the HVAC-system will provide active cooling. Now the HVAC-system is in cooling mode and the airflow rate will be increased. As soon as the temperature drops below the cooling setpoint, the cooling will stop and the airflow rate will return to normal. It is however desirable that the free cooling of the office continues to avoid the need for active cooling. Therefore the energy regime is determined from the interior temperature: as long as the interior temperature is lower than the average between the heating and cooling setpoint, the system is in heating mode. Otherwise, the system is in cooling.

Table 2 shows the heating and cooling demand as a function of the maximum allowed airflow rate. During night-time and weekends, the controller is disabled. During heating demand, the minimal ventilation rate is chosen and the heating demand hardly changes compared to the base case AFW. During cooling conditions, the airflow rate is increased whenever useful. Hence, the cooling demand may be reduced by up to 45 % without changing the heating demand. As for the previous case, it should be noted that the cooling effect is mainly caused by free cooling.

As a further step to save heating energy, recuperation of the return air is implemented. Recuperation tries to lower the energy demand by reusing that part of the return air which is not needed for ventilation. Only when the total airflow rate exceeds the required ventilation airflow rate, recuperation of the AFW return air is possible. On top of the speed adjustable fan and the diaphragms, a mixing chamber allowing recuperation should be added to the HVAC-system. As the northeast and southwest facades have a different thermal behaviour, the system is able to control both orientations separately.

Previous studies have shown that always recuperating the AFW return air increases both the heating and cooling demand (Saelens, 2002). An optimal recuperation strategy only recuperates whenever it is useful. The control strategy used in the presented analysis is based on the energy content of the supply air in the HVAC-system. This algorithm is able to compare the energy content of different recuperation settings for the different AFWs in the building. By using the previously mentioned AFW model, a correlation between the incoming solar radiation, the exterior temperature, the airflow rate and the outlet temperature was established and implemented in the BEMS allowing it to predict the outlet temperature of the different AFWs. At each timestep, the BEMS compares the energy content of the supply air based on the conditions during the previous timestep for different recuperation settings. Based on this information the BEMS chooses the settings which minimize the energy content of the supply air.

Table 2 shows the energy demand as a function of the maximum allowed recuperation airflow rate. A reduction of the heating demand up to 20 % is now possible. It may also be noted that the cooling demand decreases with approximately 5 %.

A logical step to optimize both the heating and cooling demand is combining the airflow rate control and recuperation strategy. Both the heating and cooling load decrease with increasing airflow rate (Table 2). The maximum heating load reduction equals 22 %, the maximum cooling load reduction is 39 %. These reductions are somewhat smaller than what is achieved when both strategies are used separately. To draw an overall conclusion it should again be noted that an increase of the airflow rate raises the fan energy. Hence, the reductions have to be weighed against this extra energy.

TABLE 2

Energy demand of AFWs.

AFW FIXED AIRFLOW RATE				
NO DISTRIBUTION FROM INTERNAL ZONE				
G_a (m³/(h.m))	**20**	**40**	**80**	**120**
QH (kWh/(m².a))	31.6	67.1	121.4	155.2
QC (kWh/(m².a))	-36.9	-24.7	-19.6	-18.6
DISTRIBUTION FROM INTERNAL ZONE				
G_a (m³/(h.m))	**20**	**40**	**80**	**120**
QH (kWh/(m².a))	30.1	63.3	112.8	142.3
QC (kWh/(m².a))	-33.7	-23.1	-18.7	-17.5
AFW CONTROLLED AIRFLOW RATE				
$G_{a,max}$ (m³/(h.m))	**20**	**40**	**80**	**120**
QH (kWh/(m².a))	31.6	30.6	30.4	31.0
QC (kWh/(m².a))	-36.9	-29.7	-26.0	-25.4
AFW RECUPERATION				
$G_{r,max}$ (m³/(h.m))	**0**	**20**	**60**	**100**
QH (kWh/(m².a))	31.6	29.4	27.3	25.4
QC (kWh/(m².a))	-36.9	-34.8	-34.8	-34.9
AFW CONTROLLED AIRFLOW RATE AND RECUPERATION				
$G_{a,max}$ (m³/(h.m))	**20**	**40**	**80**	**120**
$G_{r,max}$ (m³/(h.m))	**0**	**20**	**60**	**100**
QH (kWh/(m².a))	31.6	29.7	27.6	25.8
QC (kWh/(m².a))	-36.9	-31.1	-27.1	-26.5

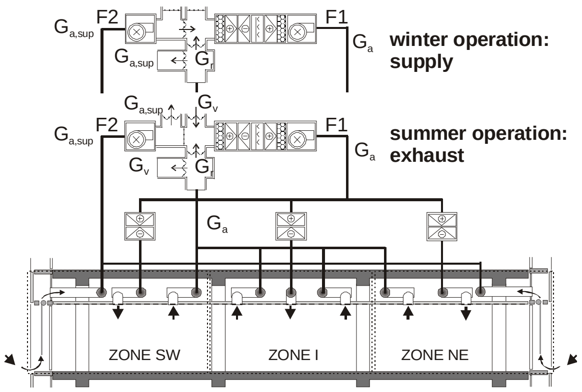

Figure 4 Schematic representation of the simulated office floor for typical SUP configurations.

Supply window (SUP)

To optimize the SUP results, important modifications to the HVAC-plant are necessary. Figure 4 gives a schematic representation of the HVAC-plant. In winter, the heating demand decreases dramatically by supplying the ventilation air for the HVAC-system through the supply window ($G_{a,sup}$ in Fig. 4). This allows to capture solar radiation and to reuse part of the transmission losses. Only one fan (F1 in Fig. 4) is operated in this situation. If necessary, part of the air can be recirculated (G_r on Fig. 4). In summer, the additional energy from the SUPs is not needed. However it may be desirable to ventilate the SUPs to prevent overheating. To achieve this, a second fan (F2 in Fig. 4) has to be operated and the mixing chamber has to be positioned in such a way that exterior air is supplied to the HVAC-plant instead of air coming from the SUPs (Fig. 4). Three operation modes are analyzed (1) always recuperation, (2) controlled recuperation and (3) controlled recuperation and free cooling.

In case of the “always recuperation” mode, the supply air for the HVAC-plant is supplied by the SUP at all times. The base case is variant a variant of this case. Also the airflow for the internal zones is supplied through the SUPs. As a consequence the airflow rate in the SUPs is 50% higher than the airflow rate in the zones ($G_{a,sup}$ = 1.5 x G_a). The airflow rate and HVAC-settings are fixed throughout the year. Recirculation is disabled (G_r = 0 in Fig. 4). The optimal airflow rate through the SUPs equals the ventilation airflow rate (Table 3). Both the heating and cooling load increase when the airflow rate through the SUPs increases. The heating demand rises because the energy content of the return air drops with increasing airflow rate and concurrently the cavity is colder which increases the transmission losses. During cooling conditions, the energy content increases with increasing airflow rate. This negative effect is not countered by the lower cavity temperature which lowers with increasing airflow rate.

In the controlled recuperation case, the BEMS can extract the supply air for the HVAC-system from the exterior environment or from the SUPs. As long as the system is in heating mode, the supply air is provided through the SUPs and equals the hygienic ventilation rate (including the ventilation air needed for the internal zones) (Fig. 4). The definition of the heating and cooling mode is the same as for the AFWs. Furthermore the system may increase the airflow rate in the SUPs to $G_{a,sup,max}$ in order to take advantage of high outlet temperatures. Note that this maximum airflow rate equals 1.5 x $G_{a,max}$ because the internal zone has to be ventilated as well. As for the AFWs, this control is based on the energy content of the return air rather than on the temperature of the return air. If the system is in cooling mode (Fig. 4, summer operation), the BEMS closes the connection between the SUPs and the HVAC-system. The airflow rate through the SUPs of zones with cooling equals the maximal airflow rate ($G_{a,sup}$ = $G_{a,sup,max}$). The supply air to the HVAC-system equals the buildings ventilation airflow rate (G_a = G_v). Note that the SUPs now are ventilated with the second fan.

Implementing this controlled recuperation strategy proofs to be a successful approach (Table 3). The heating load decreases because of the recuperation algorithm. As for the airflow windows, the heating demand decreases if a higher recuperation rate is allowed. The gains should be weighed against the increase of the fan energy.

The cooling demand decreases considerably because the warm return air from the SUPs is no longer recovered. As the cooling demand hardly depends on the airflow rate through the supply window, these results also show that the influence of the airflow rate on the transmission gains during summer conditions is relatively small. This was to be expected as the thermal resistance of the inner pane window is high.

In order to further lower the cooling load, free cooling is added to the controlled recuperation case. If the system is in cooling mode, the supply airflow rate to the HVAC-system (G_v) is now increased above the ventilation rate to $G_{v,max}$ if the average zone temperature is warmer than the exterior temperature. The combination of the recuperation strategy and free cooling has a minor impact on the heating demand but further lowers the cooling demand.

Table 3
Energy demand of SUPs.

SUP ALWAYS RECUPERATION				
G_a (m³/(h.m))	**20**	**40**	**80**	**120**
$G_{a,sup}$ (m³/(h.m))	**30**	**60**	**120**	**180**
QH (kWh/(m².a))	17.9	47.4	101.2	135.3
QC (kWh/(m².a))	-45.3	-49.7	-58.0	-72.5
SUP CONTROLLED RECUPERATION				
$G_{a,sup,max}$ (m³/(h.m))	**30**	**60**	**120**	**180**
QH (kWh/(m².a))	17.9	17.2	16.4	15.4
QC (kWh/(m².a))	-45.3	-17.9	-17.1	-16.7
SUP CONTROLLED RECUPERATION AND FREE COOLING				
$G_{a,sup,max}$ (m³/(h.m))	**30**	**60**	**120**	**180**
$G_{v,max}$ (m³/(h.m))	**20**	**40**	**80**	**120**
QH (kWh/(m².a))	17.9	17.3	16.4	15.5
QC (kWh/(m².a))	-45.3	-15.4	-14.2	-13.5
	BASE CASE			

Double-Skin Facades (DSF)

The optimization strategy of the naturally ventilated facade focuses on the position of the inlet and outlet apertures. The idea is straightforward. During heating mode, the apertures are closed to create an extra insulating barrier. During cooling mode, the apertures are opened to ventilate the cavity and prevent overheating. In order to automatically control the airflow in the cavity, motorized dampers, powered adjustable apertures or automated operable windows have to be installed. Three situations are possible: (1) closed openings (0 in Table 4), (2) normal openings (1 in Table 4) and (3) large openings (2 in Table 4). The pressure characteristics of the cavities with opened aperture are based on experimental data available in Saelens (2002). The situation with normal apertures represents the base case.

First we analyze the energy demand when the apertures are fixed at one position throughout the year (Table 4). Closing the cavity decreases the heating demand, while increasing the cooling load compared against the results of the base case. Maximizing the ventilation decreases the cooling load but increases the heating load.

This conflicting situation is resolved by implementing the above mentioned control mechanism. Increasing the maximum airflow rate in summer proves to be successful to control the cooling loads (Table 4). Allowing the system to toggle between open, normal and large opening (0-1-2 in Table 4) does not produce noticeable better results. Implementing a simple open/close algorithm proofs to be sufficient to achieve an optimal result. Finally, also free cooling of the office is implemented (0-2-F in Table 4) and combined with the control mechanism. This technique significantly lowers the cooling demand, but is not a merit of the DSF.

As an illustration, Table 4 also compares the results of the SUP where no recuperation is allowed with the results of the DSF with fixed apertures. Expectedly, the heating demand of both MSF-types is comparable. The cooling demand of the DSF is somewhat higher but there is no need for an extra fan. As a consequence the overall energy efficiency of the DSF will probably outperform that of the SUP.

Table 4
Energy demand of DSFs.

DSF FIXED GRIDS				
aperture	**0**		**1**	**2**
QH (kWh/(m².a))	34.5		36.2	36.9
QC (kWh/(m².a))	-22.2		-19.8	-18.5
DSF CONTROLLED GRIDS				
aperture	**0-1**	**0-2**	**0-1-2**	**0-2-F**
QH (kWh/(m².a))	34.4	34.3	34.3	34.0
QC (kWh/(m².a))	-20.0	-18.7	-18.7	-11.8
SUP WITHOUT RECUPERATION				
$G_{a,sup}$ (m³/(h.m))	**30**	**60**	**120**	**180**
QH (kWh/(m².a))	36.1	36.4	36.7	36.9
QC (kWh/(m².a))	-18.2	-17.7	-16.8	-16.5

Traditional Facades (IGUe and IGUi)

A comparison of the base case traditional facades against the optimized MSFs shows that the optimization provides a considerable improvement of the MSF heating demand (Fig. 5). Only the heating demand of the DSF does not improve very much. Except for the AFW, also the cooling demand of the optimized MSFs outperforms the cooling demand of the IGUe (Fig. 5). From an energy point of view, the optimized multiple-skin facades may compete with the non-optimized traditional facade systems.

It can be argued that this is no longer a fair comparison if the energy performance of the IGUs is not also optimized. Therefore we implement three optimization strategies: (1) a heat exchanger (HE) to decrease the ventilation energy, (2) night time ventilation (NV) and (3) free cooling (FC) to temper the cooling demand.

In order to recover part of the ventilation energy, a cross-flow heat exchanger system is positioned between the supply and exhaust ducts. As a result the heating demand decreases considerably (Table 5, HE). Due to the heating of the supply air when the exterior temperature is higher than the exhaust temperature, the cooling demand somewhat raises. For a Belgian climate, the effect is rather limited (Table 5, HE).

The algorithm for night ventilation increases the ventilation during night-time whenever the maximum zone temperature of the previous day surpassed the average between the setpoint for heating and cooling and the instantaneous exterior temperature is lower than the instantaneous interior temperature. To avoid the need to turn on the heating during the morning, the night-ventilation is turned off as soon as the zone temperature drops below the setpoint for heating. The algorithm is able to control each zone separately. This ensures a maximal cooling of each zone and minimizes the fan energy. As a consequence, the cooling demand now decreases substantially (Table 5, NV). Despite the temperature cut-off for ventilation there is a small raise of the heating demand.

If the building is in cooling mode and the exterior temperature is lower than the interior temperature the building is intensively ventilated. Implementation of free cooling decreases the cooling load and hardly changes the heating demand (Table 5, FC).

Optimizing both the heating and cooling demand is achieved by combining the heat-exchanger and the night-time ventilation (Table 5, HE+NV). Implementation of free cooling further decreases the cooling load without changing the heating demand (Table 5, H+N+FC).

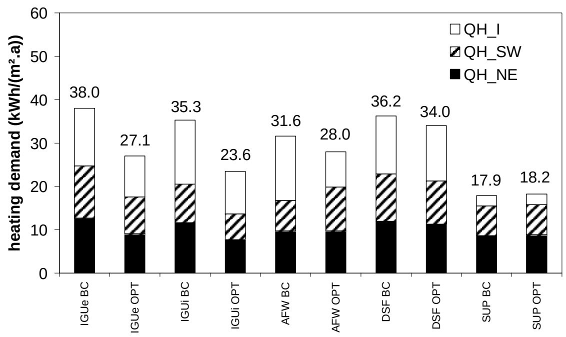

a. Heating demand

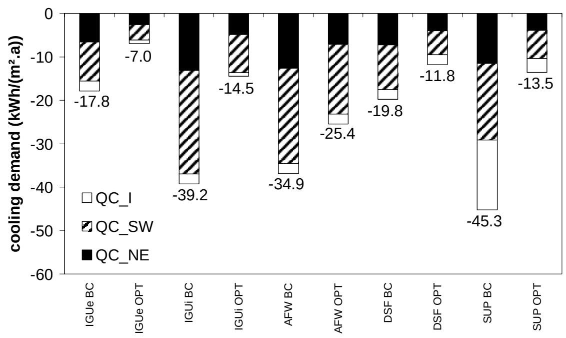

b. Cooling demand

Figure 5 Energy demand of non-optimized base case facades (BC) compared against optimized variants (OPT).

Table 5
Energy demand of IGUs.

IGUE			
case	**BC**	**HE**	**NV**
QH (kWh/(m².a))	38.0	26.0	38.4
QC (kWh/(m².a))	-17.8	-22.1	-9.8
case	**FC**	**HE+NV**	**H+N+FC**
QH kWh/(m².a))	38.2	27.0	26.6
QC (kWh/(m².a))	-11.6	-10.1	-7.0
IGUI			
case	**BC**	**HE**	**NV**
QH (kWh/(m².a))	35.3	23.0	35.7
QC (kWh/(m².a))	-39.2	-43.9	-22.0
case	**FC**	**HE+NV**	**H+N+FC**
QH kWh/(m².a))	35.5	23.5	23.6
QC (kWh/(m².a))	-25.1	-22.7	-14.5
Legend: BC = base case, HE = heat exchanger, NV = N= night ventilation, FC = F = free cooling			

CONCLUSIONS

In this paper, different strategies to optimize the energy efficiency of multiple-skin facades are studied and compared against the results of traditional cladding systems. By implementing control strategies the energy efficiency of all facade systems is significantly improved. Using an algorithm based on the energy content of the return air, recuperation of the air returning from the airflow window and supply window is useful to lower the heating demand. For the naturally ventilated double-skin facade controlled apertures are beneficial. A simple open-close strategy proofs to be sufficient. Controlling the airflow rate is a successful approach to lower the cooling demand for all facade typologies. In most cases the cooling is caused by free cooling rather than being a merit of the multiple-skin facades.

The supply window has the highest potential to benefit from the optimization techniques. It is able to considerably reduce the heating demand while providing an acceptable cooling demand. The traditional facade with exterior shading device, however, still provides the best solar protection. The double-skin facade is also able to efficiently control the cooling demand but is limited to improve the heating demand. The airflow window is capable of significantly lowering the heating demand but still suffers from high cooling demands.

ACKNOWLEDGMENTS

This research is funded by a grant of the Flemish Institute for the Promotion of Industrial Scientific and Technological Research (IWT: Vlaams Instituut ter Bevordering en Promotie van het Wetenschappelijk-Technologisch Onderzoek in de Industrie). Their financial contribution is gratefully acknowledged.

REFERENCES

Compagno, A. 1995, Intelligent Glass Facades.- Material, Practice, Design, Basel: Verlag für Architektur.

Gratia E., De Herde, A. 2004. Natural cooling strategies efficiency in an office building with a double-skin facade. Energy and Buildings, Vol. 36, pp. 1139 – 1152.

Haddad, K.H., Elmahdy, A.H. 1998, Comparison of the Monthly Thermal Performance of a Conventional Window and a Supply-Air Window, ASHRAE Transactions, Vol. 104, Part 1B: 1261-1270.

Manz, H., Simmler, H. 2003, Experimental and numerical study of a mechanically ventilated glass double facade with integrated shading device. Proc. of Research in Building Physics Conference, Leuven, Belgium, pp. 519-526.

Müller, H., Balowski, M. 1983, Waste Air Ventilated Windows for Offices, Heizung Luftung Haustechnik, Vol. 34, n° 10: 412-417.

Oesterle, E., Lieb, R.-D, Lutz, M. and W. Heusler 2001, Double-Skin Facades. – Integrated Planning, Munich: Prestel.

Poirazis, H. 2004, Double skin facades for office buildings. Literature review, Dept. of Construction and Architecture, Lund University.

Saelens, D. 2002. Energy performance assessment of single storey multiple-skin facades. Ph.D. dissertation, K.U.Leuven, Leuven, Belgium.

Saelens, D., Roels, S., Hens, H. 2004, Optimization of the energy performance of airflow windows, Proc. of Performance of Exterior Envelopes of Whole Buildings IX, Florida, USA.

Safer, N., Woloszyn, M., Rusaouen, G., Roux, J-J. 2004, Numerical studies with CFD approach of the heat and air flow transfers combined with solar radiation in double-skin facades. The 21th Conference on Passive and Low Energy Architecture, Eindhoven, The Netherlands.

Stec W.J., van Paassen, A.H.C. 2005, Symbiosis of the double skin facade with the HVAC system, Energy and Buildings, Vol. 37, pp. 461 – 469.

TRNSYS, 2000, TRNSYS: A Transient Simulation Program, Reference Manual, Wisconsin: Solar Energy Lab, Univ. of Wisconsin-Madison.